LAWRENCE
LIVERMORE
NATIONAL
LABORATORY

UCRL-JRNL-207520

The Effect of Organic Ligand Binding on the Growth CdSe Nanoparticles Probed by Ab-Initio Calculations

A. Puzder, A. J. Williamson, N. Zaitseva, G. Galli, L. Manna, A. P. Alivisatos

October 27, 2004

Nanoletters

The Effect of Organic Ligand Binding on the Growth CdSe Nanoparticles Probed by Ab-Initio Calculations

Aaron Puzder, Andrew J. Williamson,* Natalia Zaitseva, and Giulia Galli
Lawrence Livermore National Laboratory, Livermore, CA 94550

Liberato Manna† and A. Paul Alivisatos
Lawrence Berkeley Laboratory, Berkeley, CA

First principles electronic structure simulations are used to study the atomistic detail of the interaction between organic surfactant molecules and the surfaces of CdSe semiconductor nanoparticles. These calculations provide insights into the relaxed atomic geometry of organics bound to semiconductor surfaces at the nanoscale as well as the electronic charge transfer between surface atoms and the organics. We calculate the binding energy of phosphine oxide, phosphonic and carboxylic acids and amine ligands to a range of CdSe nanoparticle facets. The dominant binding interaction is between oxygen atoms in the ligands and cadmium atoms on the nanoparticle surfaces. The most strongly bound ligands are phosphonic acid molecules, which bind preferentially to the facets forming the sides of CdSe nanorods. The calculated relative binding strengths of ligands to different facets support the hypothesis that these binding energies control the relative growth rates of different facets, and therefore the resulting geometry of the nanoparticles.

Over the last decade, dramatic progress has been made synthesizing semiconductor quantum dots using colloidal chemistry techniques. In particular, the procedure for synthesizing CdSe quantum dots has been refined to the point where commercial quantities of dots with controlled sizes and optical properties can be routinely produced[1–4]. These advances in synthesis have led to the adoption of CdSe nanostructures in a range of technological applications including fluorescent probes for biological imaging[5, 6], solar cells [7], and quantum dot lasers [8]. Recently, controlled growth of nanoparticles with asymmetric geometries such as rods, rice grains, teardrops, arrowheads, and branched multi-pod structures[9–13] have also been refined by controlling monomer and ligand concentrations[11, 12]. The ability of these asymmetric shapes to align and self-assemble may lead to additional applications such as magnetic information storage[14].

While the success of these synthesis techniques is indisputable, we still lack a detailed understanding of the processes controlling the growth of crystalline CdSe quantum dots and rods and the passivation of their surfaces with organic ligands. Several fundamental questions exist, such as: (i) What is the atomistic structure of the center and the surface of CdSe quantum dots? (ii) What is the nature of the interface between the dots and the surface ligands? (iii) Which ligands bind most strongly to which surface facets? and (iv) In the light of recent evidence indicating a dependence of nanoparticle geometry on ligand concentrations[10, 12], what is the mechanism by which ligands control the shape and growth direction of the nanoparticles? Answering such questions and improving our understanding of these synthesis processes at the atomistic level is a valuable step towards the ultimate goal of designing nanostructures from the bottom up, with tailored structural and optical properties.

In this letter we report the results of *ab-initio* electronic structure simulations designed to provide a microscopic description of the interaction between CdSe quantum dots and organic ligands during synthesis. We simulate both the semiconductor CdSe core and the organic surfactants within the same quantum mechanical approach to obtain a complete description of the crystalline core structure, the inorganic/organic interface between the core and the surfactants, and the binding energy of the surfactants to the facets of model CdSe nucleation seeds. These calculations provide information that cannot be obtained from electron microscopy or optical spectroscopy as the organic surfactants are typically too light to image via TEM and optical spectroscopy has proved relatively insensitive to the surfactants and their interaction with the semiconductor core. By analyzing the relative binding energies of ligands to different facets of CdSe quantum dots, we provide evidence to support the recent hypothesis that those facets most strongly bound to ligands are the slowest to grow. This suggests that the geometry of nanoparticles can be controlled by altering the concentration of surfactants[10, 12].

Developing a theoretical model of II-VI colloidal quantum dot structures represents a formidable challenge to state-of-the-art, first-principles electronic structure techniques. To date, the majority of first principles quantum dot studies have concentrated on group IV (e.g. silicon[15, 16], germanium[17, 18] and carbon[19]) systems where the electronic structure of the semiconductor core can be described in terms of the s and p valence electrons and the dangling bonds at the surface can be effectively passivated with covalently bonded hydrogen atoms[20]. In contrast, we have recently demonstrated that a full quantum mechanical description of CdSe nanoparticles must include the s, p and d valence electrons to correctly determine the crystal structure of the semiconductor core and surface atoms[21]. In addi-

tion, the subtle interaction between the core and its organic surfactants is central to the properties of the dots and therefore any realistic model must also provide a full quantum description of these bonds.

Previous models of CdSe dots have represented the semiconductor core using semi-empirical tight-binding[22, 23] and pseudopotential[24] approaches, where the atomic positions were fixed to bulk CdSe and the organic surfactants passivating the surface were represented either by simple model potentials or single oxygen atoms. These semi-empirical approaches cannot calculate atomic forces and are therefore unable to model the actual core structure; they are unable to describe the electron transfer between organic ligands and the quantum dot; and most importantly, they are not reliable as total energy calculations and are thus incapable of determining relative binding energies. Here we remove these restrictions by performing first-principles electronic structure calculations to calculate the minimum energy structures of CdSe quantum dots, including their surfactants.

Our *ab initio* calculations were performed using a planewave implementation[25] of density functional theory. Periodic supercells were chosen with at least 10 Å between replica to remove spurious periodic interactions. Norm-conserving pseudopotentials were used to represent the ionic cores. In cases involving charged systems, we doubled the supercell size and used a truncated Coulomb potential for electronic interactions at distances larger than the size of the original supercell used for neutral systems. All structures were calculated using 18 Cd ($4p^6 4d^{10} 5s^2$) and 6 Se ($4s^2 4p^4$) valence electrons. The *d*-electrons in Cd were deemed necessary to generate the correct structures compared with an all-electron calculation[21]. The non-local pseudopotential contribution for Cd required the use of a quadrature integration technique to avoid possible incorrect solutions produced by, e.g. a Kleinmann-Bylander construction of the pseudopotential. Two representative wurtzite Cd_xSe_x clusters were studied with $x = 15$, and 33, which have diameters of 1.1, and 1.3 nm. Each cluster was initially constructed on a wurtzite lattice with bulk Cd-Se bond lengths and then relaxed to its lowest energy configuration. The initial and relaxed structures of the $Cd_{33}Se_{33}$ cluster are shown in Fig 1. The relaxation of these clusters from the ideal wurtzite structure to their lowest energy configuration is discussed in Ref.[21], where it was shown that the ideal wurtzite structure of CdSe quantum dots is unstable with respect to surface relaxations. Additionally, these surface relaxations were shown to be the origin of the large intrinsic band gap of CdSe nanoparticles.

Recently, some of us have demonstrated that the aspect ratio of CdSe dots and rods can be controlled by altering the relative concentrations of hexylphosphonic acid (HPA) and trioctylphosphine oxide (TOPO) solvents during the CdSe quantum dot growth process[10]. Similar geometric control has also been demonstrated by varying the concentration of the precursor monomers in the growth solutions[11, 12]. Both these demonstrations support a model in which growth occurs on exposed facets with no attached ligands. The fraction of time during which a facet is blocked by a ligand depends on both the concentration of the ligand in the growth solution and its binding energy on the facet. To theoretically investigate this model we have calculated the binding energy of a range of representative organic ligands to different facets of the Cd_xSe_x clusters. The ligands we considered include phosphonic acids, phosphine oxides, amines, and carboxylic acids. For each ligand, the binding to facets with Miller-Bravais indices (0001),(000$\bar{1}$), (01$\bar{1}$0) and (11$\bar{2}$0) (see Fig 1) was calculated. It has been speculated that CdSe rods grow in the [0001] direction[10] (see arrow in Fig 1) and therefore these facets would correspond to the two ends and the sides of the nanorods. After each monolayer of growth the (0001) and (000$\bar{1}$) facets are either Cd or Se terminated. Specifically, the (0001) facet is either terminated by Se atoms with 1 dangling bond or Cd atoms with 3 dangling bonds. Similarly, the (000$\bar{1}$) facet is either terminated by Se atoms with 3 dangling bonds or Cd atoms with 1 dangling bond. Here we assume that the surfaces terminated with 3 dangling bonds are highly chemically active and ligand binding is most likely to affect growth from the surfaces with only 1 dangling bond, i.e. Se terminated (0001) and Cd terminated (000$\bar{1}$).

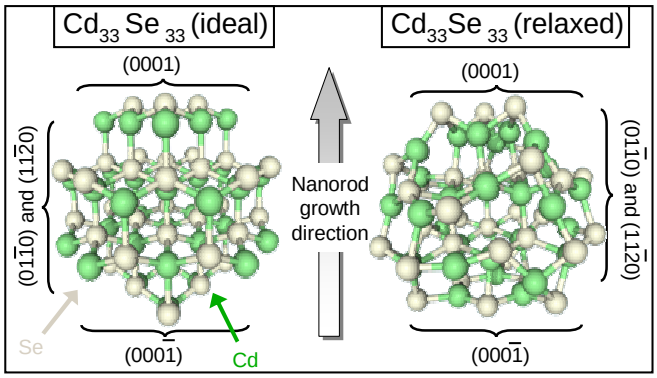

FIG. 1: Ideal wurtzite and relaxed structure of $Cd_{33}Se_{33}$ showing the (0001),(000$\bar{1}$), (01$\bar{1}$0) and (11$\bar{2}$0) facets to which ligands are attached. Cd (Se) atoms are shown in green (gray).

In addition to calculating binding energies of various ligands to each of these facets, we also performed relaxations with initial configurations of the ligands at a number of different points on the surface. For example, when both surface Cd and Se were available for binding, we started independent calculations with the ligand bound to each. To reduce the computational cost of calculating the ligand binding energies, we reduced

	$Cd_{15}Se_{15}$		$Cd_{33}Se_{33}$			
	$(000\bar{1})$	(0001)	$(000\bar{1})$	(0001)	$(01\bar{1}0)$	$(11\bar{2}0)$
Ligand	Cd	Se	Cd	Se	Cd/Se	Cd/Se
PO	1.06	0.66	0.85	0.63	1.23	1.37
PA	1.12	0.66	1.11	0.67	1.45	1.26
CA	0.68	0.42				
TMA	0.91	1.05				

TABLE I: Calculated binding energies of phosphine oxide (PO), phosphonic acid (PA), carboxylic acid (CA) and trimethylamine (TMA) ligands to the (0001),$(000\bar{1})$, $(01\bar{1}0)$ and $(11\bar{2}0)$ facets of $Cd_{15}Se_{15}$ and $Cd_{33}Se_{33}$ quantum dots. All binding energies in eV.

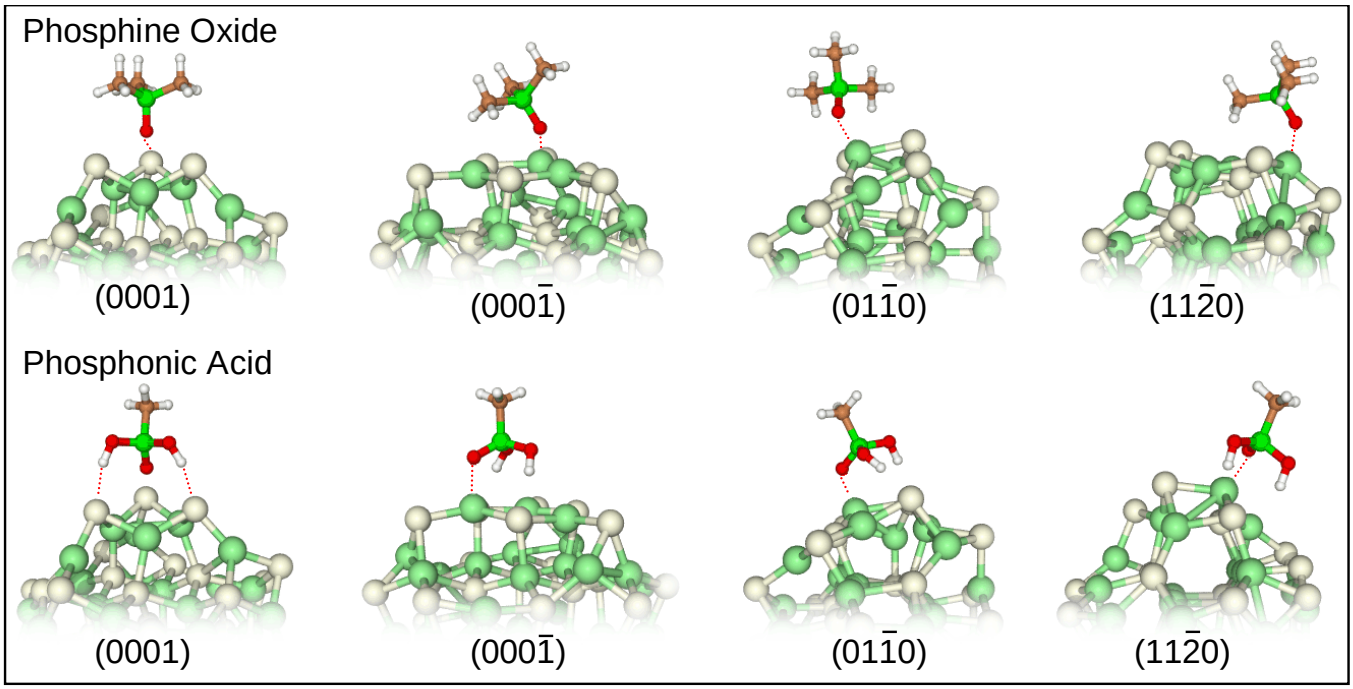

FIG. 2: Calculated structures of phosphine oxide and phosphoric acid molecules bound to the (0001),$(000\bar{1})$, $(01\bar{1}0)$ and $(11\bar{2}0)$ facets of a $Cd_{33}Se_{33}$ quantum dot. Cd, Se, O, P, C and H atoms are colored green, gray, red, green, brown and white respectively.

the length of the alkane chains in the phosphine oxides, phosphonic and carboxylic acids and amines representing the TOPO, HPA and carboxylic acids used in conventional CdSe synthesis. Approximating the alkane chains with hydrogen atoms, i.e. approximating TOPO with H_3PO and HPA with $H(OH)_2PO$ was found to be insufficient to represent the electronic structure of the band edge states or the magnitude of the binding energy. However, replacing the alkane chains with a single methyl group, producing tri-methyl phosphine oxide $(CH_3)_3PO$, mono phosphonic acid $CH_3(OH)_2PO$, acetic acid, CH_3COOH, and trimethyl-amine $(CH_3)_3N$ was sufficient to accurately represent the band edge states and band gap of the larger chain ligands. In representative tests, these single C atom ligands produced nearly identical binding energies (within 0.01 eV) to their full chain equivalents. In all the following calculations these single C atom chain ligands are used and are referred to as phosphine oxide (PO), phosphonic acid (PA), carboxylic acid (CA) and trimethylamine (TMA).

Each ligand-CdSe composite system was relaxed to its lowest energy configuration. In each case, the capping ligand always sought out its most stable configuration, i.e., a ligand that preferred to bind with a surface Cd always found the nearest Cd with which to bind, even when initially bound to a surface Se. The binding energy is defined as the difference between the combined total energies of the individual cluster and ligand and the total energy of the bound system. Initial configurations with the Cd_xSe_x cluster in both the ideal wurtzite structure and the relaxed structures calculated in Ref.[21] were also tested. The final relaxed geometries of the [cluster+ligand] system were generally found to be independent of the starting geometry, suggesting there are

no kinetic barriers limiting the relaxation of the ligands into their lowest energy configurations. The relaxation of the Cd_xSe_x cluster was also found to be relatively insensitive to the presence of organic ligands, as described in Ref.[21].

Table I shows the calculated binding energies of PO, PA, CA, and amines to the (0001),(000$\bar{1}$) facets of $Cd_{15}Se_{15}$ and the (0001),(000$\bar{1}$), (01$\bar{1}$0) and (11$\bar{2}$0) facets of the $Cd_{33}Se_{33}$ quantum dots. The relaxed structures of PO and PA bound to the (0001),(000$\bar{1}$), (01$\bar{1}$0) and (11$\bar{2}$0) facets of the $Cd_{33}Se_{33}$ dot are shown in Fig. 2. All the density functional binding energies shown in Table I were calculated with the standard local density (LDA) functional. Representative calculations were repeated with the gradient corrected PBE functional. The PBE calculated binding energies show the same relative binding strengths between facets for a given ligand and also the same relative binding strengths of different ligands on the same facet. The absolute PBE calculated binding energies are 40-50% smaller than the LDA values as is typically found.

Table I shows that both PO and PA molecules bind most strongly to the apolar (01$\bar{1}$0) and (11$\bar{2}$0) facets on the "sides" of the quantum dots and rods. Analysis of the geometry of the relaxed (01$\bar{1}$0) and (11$\bar{2}$0) dot surfaces bound to PA and PO (see Fig. 2) shows that the binding always occurs between the oxygen atom, double bonded to the phosphorus in the PA and PO molecules and a Cd atom on the surface of the dot. Similarly, in the CA calculations (structures not shown) the binding is between the oxygen double bonded to the carbon in the acid and the surface Cd. Simulations in which the oxygen in PA, PO and CA were initially aligned next to a Se atom on the (01$\bar{1}$0) and (11$\bar{2}$0) surfaces found that the PA, PO and CA molecules relax directly into lower energy configurations where the oxygen hops to the nearest Cd on the surface.

Table I shows that PO and PA molecules bind more strongly to the Cd covered polar (000$\bar{1}$) surfaces than the Se covered (0001) surfaces. Analysis of the geometry of these relaxed structures shows that again the PO and PA bind to the Cd (000$\bar{1}$) surfaces via an oxygen atom to surface Cd. However, this oxygen binds to (0001) Se surface atoms more weakly so that the orientation of the ligand is primarily governed by the hydrogen atoms in the OH groups on the PA molecules. For both PO and PA molecules, the binding to the (000$\bar{1}$) and (0001) surfaces is weaker than the binding to the (01$\bar{1}$0) and (11$\bar{2}$0) surfaces. This could result from the fact that the Cd atoms to which the ligands bind are 3-fold coordinated on the (000$\bar{1}$) surface, while, as a result of curvature, the Cd atoms on the (01$\bar{1}$0) and (11$\bar{2}$0) facets are only two-fold coordinated. These two-fold coordinated Cd atoms are less constrained than the 3-fold coordinated Cd atoms and are able to transfer more charge into a bond with the ligand.

The relative binding strength of PO and PA molecules to the different facets of CdSe nanoparticles is similar for the two sizes of cluster, $Cd_{15}Se_{15}$ and $Cd_{33}Se_{33}$, studied here. This suggests that these results can be extrapolated to make qualitative predictions of the binding energies of these molecules to the larger 2-5 nm nanoparticles that are typically synthesized. However, the structures do appear to gain some additional stability by taking advantage of the high radius of curvature present on these nanoscale surfaces. The structures of PO and PA molecules bound to (01$\bar{1}$0) and (11$\bar{2}$0) facets shown in Fig. 2 show that the molecules rotate away from the surface, similar to the reconstructed surfaces of silicon nanostructures[20].

To investigate the effect of charging, we repeated a representative set of the above calculations, replacing the PA molecule with PA^- and PA^{2-}. For CdSe synthesis procedures using CdO as the Cd precursor, it is expected that the Cd^{2+} ion is dissolved by 2 HPA^- molecules. For syntheses using the $Cd(CH_3)_2$ precursor the Cd ion is immediately free upon injection and may not require charged HPA to solvate it. Our calculations find that the surface binding of charged PA is, as expected, significantly stronger than neutral PA, for example, the binding energy of PA^- to the Cd (000$\bar{1}$) surface is 3 eV compared to 1.12 eV for neutral PA. However, we find that the relative binding strengths of PA^- to different facets are the same as neutral PA, i.e. it binds most strongly to (01$\bar{1}$0) and (11$\bar{2}$0) sides, then the Cd (000$\bar{1}$) surface and most weakly to the Se (0001) surface. The PA^{2-} molecule binds aggressively to all surfaces. On the Se (0001) surface it actually binds to Cd atoms in the sub-surface layer, significantly distorting the surface structure.

Based on these calculations, we clearly see that on the facets perpendicular to the c-axis, both PO and PA bind more strongly to the (000$\bar{1}$) than the (0001) surface and even more strongly to the facets along the c-axis. Furthermore, we find the binding to be stronger for PA ligands than PO ligands suggesting HPA can in fact facilitate nanorod growth and that this growth occurs on the Cd dominated (000$\bar{1}$) facet. We note that these relative binding energies occur whether we use LDA or GGA and that they occur regardless of whether the PA is charged or not.

To investigate the effect of switching from phosphorus based ligands, we also calculated the binding energy of amines and carboxylic acids to the CdSe nanoparticles surfaces. Table I also shows the calculated binding energies of trimethylamine to the (0001) and (000$\bar{1}$) facets of the $Cd_{15}Se_{15}$ quantum dot. Analysis of the relaxed structures (not shown) shows that the binding occurs between the lone pair of electrons on the nitrogen atom and the Cd and Se atoms on the surface. Interestingly, trimethylamine is the only ligand which is more strongly bound to Se terminated surfaces than Cd terminated surfaces. While the difference in binding energies is small, this re-

versal in binding preference might suggest that CdSe rods grown in high concentrations of amine solutions will grow from the Cd terminated $(000\overline{1})$ facet rather than the Se terminated (0001) facet, i.e. in the opposite direction to rods grown in TOPO/HPA.

Table I also shows the binding energies of CA to the (0001) and $(000\overline{1})$ surfaces of $Cd_{15}Se_{15}$ and four surfaces on $Cd_{33}Se_{33}$. We find that the binding energies to be twice as small as that in any other ligand. This smaller energy suggests a much weaker binding to the surface and thus, that growth would occur much more rapidly and uniformly. Indeed, CdSe synthesized in the presence of carboxylic acid has been shown to generate large, rapidly grown spheres[3].

In addition to the structural relaxation and charge transfer effects included in the above calculations, there are several other effects which can influence the binding strength of ligands on CdSe nanoparticle surfaces, including; (i) charging of the ligands and/or nanoparticle, (ii) steric interference between neighboring ligands on the surface, and (iii) solvation effects due to the surrounding organic solvents. While including the effects of charging increases the surface binding energy of ligands, we expect that the steric interference and solvation effects will both reduce the ligand binding energies. In particular, the three long alkane chains on each TOPO molecule repel each other, reducing the binding energy of TOPO molecules attached to neighboring Cd atoms on $(000\overline{1})$ and $(01\overline{1}0)$ and $(11\overline{2}0)$ surfaces. In contrast, HPA has only one alkane chain which is aligned approximately perpendicular to the nanoparticle surface. Therefore, while Table I shows that PA is somewhat more strongly bound to nanoparticles surfaces than PO, we anticipate that when the effect of steric repulsion between neighboring TOPO alkane chains is included, PA will be considerably more strongly bound than TOPO. This conclusion is supported by CdSe synthesis experiments in pure TOPO which demonstrate uncontrollable growth of CdSe into macroscopic pieces of material. This further suggests that the success of CdSe nanoparticle synthesis in "technical" TOPO solutions, which typically contain 10% of other organics, is due to the stronger binding of these additional organics, such as phosphonic acids, which bind more strongly to the surface, controlling the growth rate.

In conclusion, we have performed accurate, first principles electronic structure calculations of the interaction between representative organic ligands and the surfaces of CdSe nanoparticles. We find that the dominant binding is between oxygen atoms in the ligands and cadmium atoms on the nanoparticle surfaces. The most strongly bound ligands are phosphonic acid molecules, which bind preferentially to the $(01\overline{1}0)$- and $(11\overline{2}0)$-type sides of the nano-rods. The calculated relative binding energies to different facets support the hypothesis that the relative binding energies control the relative growth rates of different facets, and hence the resulting geometry of the nanoparticles. We also extended the calculations to study two alternative ligands; carboxylic acids and amines, producing interesting predictions of novel growth geometries in these solvents. These calculations demonstrate that first principles studies can be used as a powerful tool for predicting the interaction mechanisms and relative interaction strengths between organics and semiconductor nanomaterials.

This work was performed under the auspices of the U.S. Department of Energy at the University of California/Lawrence Livermore National Laboratory under Contract No. W-7405-ENG-48.

* Electronic address: williamson10@llnl.gov
† Current address: National Nanotechnology Laboratory, Via Arnesano, 73100, Lecce, Italy

[1] Murray, C.; Norris, D.; Bawendi, M. *J. Am. Chem. Soc.* **1993,** *115,* 8706.
[2] Peng, X.; Schlamp, M.; Kadavanich, A.; Alivisatos, A. *J. Am. Chem. Soc.* **1997,** *119,* 7019.
[3] Qu, L.; Peng, Z.; Peng, X. *Nano Lett.* **2001,** *1,* 333.
[4] Reiss, P.; Bleuse, J.; Pron, A. *Nano Lett.* **2002,** *2,* 781.
[5] Wu, X.; Liu, H.; Liu, J.; Haley, K.; Treadway, J.; Larson, J.; Ge, N.; Peale, F.; Bruchez, M. *Nature Biotechnology* **2003,** *21,* 41.
[6] Jaiswal, J. K.; Mattoussi, H.; Mauro, J.; Simon, S. *Nature Biotechnology* **2003,** *21,* 47.
[7] Huynh, W.; Dittmer, J.; Alivisatos, A. *Science* **2002,** *295,* 2425.
[8] Klimov, V.; Mikhailovsky, A.; Xu, S.; Malko.A.,; Hollingsworth, J.; Leatherdale, C.; Eisler, H.; Bawendi, M. *Science* **2000,** *290,* 314.
[9] Peng, X.; Manna, L.; Yang, W.; Wickham, J.; Scher, E.; Kadavanger, A.; Alivisatos, A. *Nature* **2000,** *59,* 404.
[10] Manna, L.; Scher, E.; Alivisatos, A. *J. Am. Chem. Soc.* **2000,** *122,* 12700.
[11] Peng.Z.A.,; Peng, X. *J. Am. Chem. Soc.* **2001,** *123,* 1389.
[12] Peng.Z.A.,; Peng, X. *J. Am. Chem. Soc.* **2001,** *124,* 3343.
[13] Peng, X. *Adv. Mat.* **2003,** *15,* 459.
[14] Puntes, V.; Krisman, K.; Alivisatos, A. *Science* **2001,** *291,* 2115.
[15] Puzder, A.; Williamson, A.; Grossman, J.; Galli, G. *Phys. Rev. Lett.* **2002,** *88,* 097401.
[16] Williamson, A.; Grossman, J.; Hood, R.; Puzder, A.; Galli, G. *Phys. Rev. Lett.* **2002,** *89,* 196803.
[17] Pizzagalli, L.; Galli, G.; Klepeis, J.; Gygi, F. *Phys. Rev. B* **2001,** *63,* 165324.
[18] Williamson, A.; Bostedt, C.; van Buuren, T.; Willey, T.; Terminello, L.; Galli, G.; Pizzagalli, L. *Nano Lett.* **2004,** In press.
[19] Raty, J.-Y.; Galli, G.; Bostedt, C.; van Buuren, T.; Terminello, L. *Phys. Rev. Lett.* **2003,** *90,* 037401.
[20] Puzder, A.; Williamson, A.; Reboredo, F.; Galli, G. *Phys. Rev. Lett.* **2003,** *91,* 157405.
[21] Puzder, A.; Williamson, A.; Gygi, F.; Galli, G. *Phys. Rev. Lett.* **2004,** *92,* 217401.
[22] Pokrant, S.; Whaley, K. *Eur. Phys. Journ. D* **1999,** *6,*

255.
[23] Lippens, P.; Lannoo, M. *Phys. Rev. B* **1990,** *41,* 6079.
[24] Wang, L.; Zunger, A. *Phys. Rev. B* **1996,** *53,* 9579.
[25] F.Gygi, "The GP Code", LLNL, 2004.